

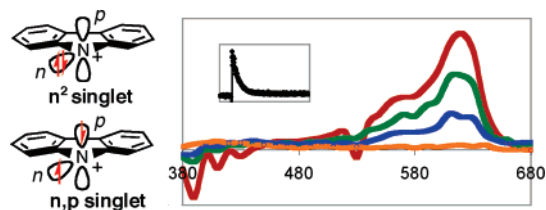
# Carbazolyl Nitrenium Ion: Electron Configuration and Antiaromaticity Assessed by Laser Flash Photolysis, Trapping Rate Constants, Product Analysis, and Computational Studies

Arthur H. Winter,<sup>†</sup> Harry H. Gibson,<sup>‡</sup> and Daniel E. Falvey<sup>\*,†</sup>

Department of Chemistry and Biochemistry, University of Maryland, College Park, Maryland 20740,  
and Department of Chemistry, Austin College, 900 North Grand Avenue, Suite 61552,  
Sherman, Texas 75090-4400

*falvey@umd.edu*

Received April 19, 2007



Laser flash photolysis of 1-(carbazol-9-yl)-2,4,6-trimethylpyridinium tetrafluoroborate generates the carbazolyl nitrenium ion ( $\tau = 333$  ns,  $k_{\text{obs}} = 3.0 \times 10^6 \text{ M}^{-1}\text{s}^{-1}$ ) having absorption bands at 570 and 620 nm in  $\text{CH}_3\text{CN}$ . The nitrenium ion is found to have reactivity comparable to structurally similar closed-shell diarylnitrenium ions, but spectroscopic evidence favors an open-shell singlet diradical assignment for the observed nitrenium ion. The carbazolyl nitrenium ion is also more reactive than diarylnitrenium ions as a likely result of antiaromatic character. *Ab initio* and hybrid DFT calculations were performed to address the degree of antiaromaticity in this and similar nitrenium ions through analysis of optimized geometries, nucleus independent chemical shifts, and isodesmic reactions.

## Introduction

Nitrenium ions are nitrogen-containing reactive intermediates of the formula  $\text{RNR}'^+$ ; they are isoelectronic to the more-familiar carbene family of intermediates and have lifetimes that seldom exceed 100  $\mu\text{s}$ .<sup>1–4</sup> Many of the studies of nitrenium ions have come as a result of evidence that aryl nitrenium ions ( $\text{Ar}-\text{N}-\text{R}^+$ ) are formed *in vivo* from enzymatic oxidation of arylamines. Due to their extreme electrophilicity, nitrenium ions add to weakly nucleophilic cellular moieties such as proteins and DNA.<sup>5–7</sup> The addition of nitrenium ions to DNA has the

potential to kill a healthy cell or begin the process to convert it into a cancerous one, and nitrenium ions have been implicated as the “ultimate carcinogen”<sup>8</sup> of certain anilines and other nitrogen-containing aromatics.<sup>9</sup> On a more positive note, nitrenium ions have also been proposed to be intermediates in the synthesis of the conducting material poly(aniline)<sup>10,11</sup> and have been exploited for useful synthetic purposes, particularly in ring-forming reactions.<sup>12–15</sup> While most of the recent work on nitrenium ion chemistry has focused on aryl nitrenium ions ( $\text{Ar}-\text{N}-\text{H}^+$ ), less attention has been given to other kinds of nitrenium ions such as alkyl nitrenium ions or nitrenium ions derived from heteroaromatic systems.

<sup>†</sup> University of Maryland.

<sup>‡</sup> Austin College.

(1) Falvey, D. E. In *Reactive Intermediates*; Moss, R. A., Platz, M. S., Maitland Jones, J., Eds.; John Wiley & Sons: New York, 2004.

(2) Falvey, D. E. *J. Phys. Org. Chem.* **1999**, *12*, 589–596.

(3) Gassman, P. G. *Acc. Chem. Res.* **1970**, *3*, 26–33.

(4) Abramovitch, R. A.; Davis, B. A. *Chem. Rev.* **1964**, *64*, 149–185.

(5) Kennedy, S. A.; Novak, M.; Kolb, B. A. *J. Am. Chem. Soc.* **1997**, *119*, 7654–7664.

(6) Thomas, S. I.; Falvey, D. E. *J. Phys. Org. Chem.* **2006**, *19*, 291–294.

(7) Famulok, M.; Boche, G. *Angew. Chem., Int. Ed. Engl.* **1989**, *28*, 468–469.

(8) Famulok, M.; Bosold, F.; Boche, G. *Angew. Chem., Int. Ed. Engl.* **1989**, *28*, 337–338.

(9) Miller, J. A. *Cancer Res.* **1970**, *30*, 1570–1579.

(10) Wei, Y.; Tang, X.; Sun, Y. *J. Polym. Sci. Part A: Chem.* **1989**, *27*, 2385–2396.

(11) Wei, Y.; Jang, G.-W.; Chan, C.-C.; Hsueh, K. F.; Hariharan, R.; Patel, S. A.; Whitecar, C. K. *J. Phys. Chem.* **1990**, *94*, 7716–7721.

(12) Waldrop, D. J.; Basak, A. *Org. Lett.* **2001**, *3*, 1053–1056.

(13) Abramovitch, R. A.; Ye, X.; Pennington, W. T.; Schimek, G.; Bogdal, D. J. *Org. Chem.* **2000**, *65*, 343–351.

(14) Abramovitch, R. A.; Ye, X. *J. Org. Chem.* **1999**, *64*, 5904–5912.

(15) Waldrop, D. J.; Zhang, W. *Org. Lett.* **2001**, *3*, 2353–2356.

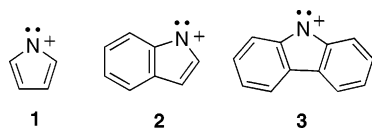


FIGURE 1. Endocyclic nitrenium ions.

To distinguish between nitrenium ions with the formally cationic nitrogen located outside of a ring and those with the cationic nitrogen contained within a ring, we use the term *endocyclic* nitrenium ions to describe nitrenium ions with the formally cationic nitrogen contained within a ring (e.g., all nitrenium ions in Figure 1), and *exocyclic* nitrenium ions for those with the formal nitrenium center outside of a ring (e.g., Ph–N–H<sup>+</sup>).

We were particularly interested in the structures of the *endocyclic* nitrenium ions shown in Figure 1 because each possibly has antiaromatic character. The cyclopentadienyl cation is one of the most well-known antiaromatic ring systems, and it has a recorded ESR triplet spectrum.<sup>16</sup> The pyrrolyl nitrenium ion **1** is its nitrenium ion analogue and the indolyl nitrenium ion **2** and the carbazolyl nitrenium ion **3** both contain this formally antiaromatic core. While the carbocation analogues of **1–3** have seen extensive studies and debate regarding the degree of antiaromaticity in these cations,<sup>16–22</sup> the nitrenium ions **1–3** have received little study.<sup>23–25</sup> Moreover, we were intrigued by the possibility for unusual ground state or low-energy electron configurations in these nitrenium ions that may be favored to avoid any antiaromatic character present in their closed-shell singlet configurations.

For any nitrenium ion, three possibilities for the electronic configuration of the singlet state are typically considered (see Figure 2).<sup>2</sup> The only electron configuration of the singlet state that has been observed experimentally is the n<sup>2</sup> singlet state, in which both of the electrons reside in a hybridized nonbonding n orbital. An open shell n,p singlet configuration and a closed shell p<sup>2</sup> configuration are usually ruled out on principle because they put electrons into a higher energy p orbital. In the cases of structures **1**, **2**, and **3**, however, certain energetic advantages can be envisaged for both of these configurations that might compensate for placement of the electrons in higher energy orbitals. For example, in both the p<sup>2</sup> singlet state and the open shell n,p singlet state any antiaromaticity (if present) is avoided. Moreover, the p<sup>2</sup> singlets may have the added stabilization of additional aromatic character.

Additionally, one expects that each of these three configurations for the singlet state should exhibit different reactivity. Typical closed shell n<sup>2</sup> singlet aryl nitrenium ions react with

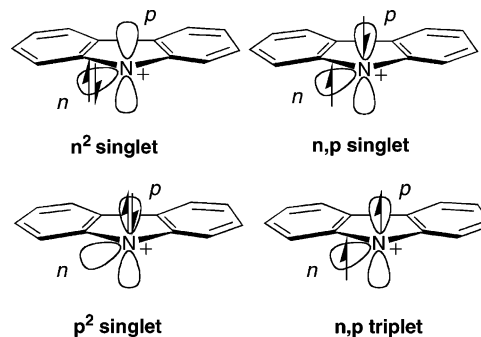


FIGURE 2. Possible electronic configurations for carbazolyl nitrenium ion.

nucleophiles at the ortho and para sites of the phenyl rings (addition to nitrogen is sometimes observed with certain pi nucleophiles). Little is known of the reactivity of open-shell n,p singlet states for carbenes or nitrenium ions, but intuition suggests that they would likely react more like diradicals than typical closed-shell singlet species. Likewise, little is known of p<sup>2</sup> singlet states for carbenes or nitrenium ions (certain palladadiphosphanyl carbenes<sup>26</sup> are thought to be p<sup>2</sup> singlets), but a p<sup>2</sup> singlet nitrenium ion would be anticipated to react like an aryl or vinyl carbenium ion, with exclusive nucleophile addition at the cationic nitrogen (which cannot delocalize the charge through resonance like the n<sup>2</sup> singlet can). All of the known examples of triplet nitrenium ions react by hydrogen atom transfer mechanisms, usually to form the reduced amine as the ultimate photoproduct.

We chose the carbazolyl nitrenium ion **3** as the best candidate for experimental studies. As a result of its greater conjugation, we anticipated that it would be longer lived and have more favorable absorption properties than **1** and **2** and, thus, have a greater chance of direct observation using our LFP system.

## Discussion/Results

**Generation of the Nitrenium Ion.** The carbazolyl nitrenium ion was generated by photolysis of 1-(carbazol-9-yl)-2,4,6-trimethylpyridinium tetrafluoroborate **4a** as shown in Scheme 1. Upon absorption of ultraviolet light, *N*-aminopyridinium salts are known to undergo heterolytic N–N bond scission to generate the nitrenium ion and the pyridine derivative **5**.<sup>27–29</sup> Barring rapid intersystem crossing of the excited singlet state of the pyridinium salt precursor **4** to its excited triplet state prior to N–N bond scission, nitrenium ions generated from these precursors are initially made in a singlet state, irrespective of whether this configuration is the ground state electron configuration.

Upon laser flash photolysis (LFP) of **4a**, a short-lived species ( $\tau = 333$  ns,  $k_{\text{obs}} = 3.0 \times 10^6 \text{ M}^{-1}\text{s}^{-1}$ ) having absorption bands at 570 and 620 nm was observed (Figure 3). Upon the basis of diagnostic LFP studies, chemical trapping experiments, and

(16) Saunders, M.; Berger, R.; Jaffe, A.; McBride, J. M.; O'Neill, J.; Breslow, R. J. M.; Hoffman, J. J. *Am. Chem. Soc.* **1973**, *95*, 3017–3018.

(17) Amyes, T. L.; Richard, J. P.; Novak, M. J. *Am. Chem. Soc.* **1992**, *114*, 8032–8041.

(18) Allen, A. D.; Tidwell, T. T. *Chem. Rev.* **2001**, *101*, 1333–1348.

(19) Breslow, R.; Chang, H. W.; Hill, R.; Wasserman, E. *J. Am. Chem. Soc.* **1967**, *89*, 1112–1119.

(20) Allen, A. D.; Fujio, M.; Mohammed, N.; Tidwell, T. T.; Tsuji, Y. *J. Org. Chem.* **1997**, *62*, 246–252.

(21) Herndon, W. C.; Mills, N. S. *J. Org. Chem.* **2005**, *70*, 8492–8496.

(22) Jiao, H.; Schleyer, P. v. R.; Mo, Y.; McAllister, M. A.; Tidwell, T. T. *J. Am. Chem. Soc.* **1997**, *119*, 7075–7083.

(23) Sparrapan, R.; Eberlin, M. N.; Augusti, R. *Rap. Comm. Mass Spectrom.* **2005**, *19*, 1775–1778.

(24) Bogdal, D. *Heterocycles* **2000**, *53*, 2679–2688.

(25) Bogdal, D. *ARKIVOK* **2001**, *6*, 109–115.

(26) Vinolle, J.; Gornitzka, H.; Maron, L.; Schoeller, W. W.; Bourissou, D.; Bertrand, G. *J. Am. Chem. Soc.* **2007**, *129*, 978–985.

(27) Abramovitch, R. A.; Evertz, K.; Huttner, G.; Gibson, H. H.; Weems, H. G. *J. Chem. Soc. Chem. Comm.* **1988**, 325–327.

(28) Winter, A. H.; Thomas, S. I.; Kung, A. C.; Falvey, D. E. *Org. Lett.* **2004**, *6*, 4671–4674.

(29) McIlroy, S.; Falvey, D. E. *J. Am. Chem. Soc.* **2001**, *123*, 11329–11330.

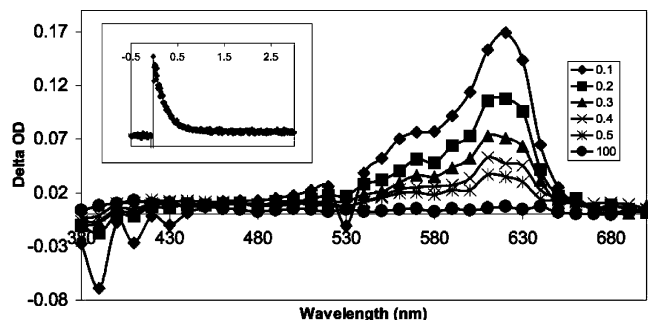
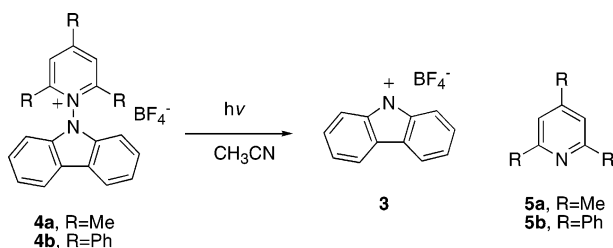


FIGURE 3. LFP of **4a** in  $\text{CH}_3\text{CN}$ . Time scale in  $\mu\text{s}$ . (Inset) Waveform at 620 nm.

#### SCHEME 1. Generation of the Carbazolyl Nitrenium Ion



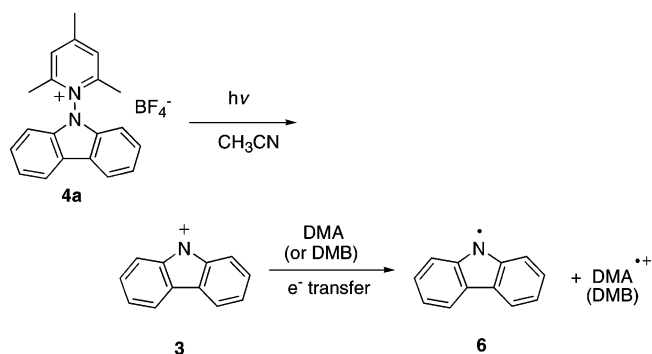
product analyses discussed below, we assign this transient to the singlet carbazolyl nitrenium ion **3**.

**Evidence for a Nitrenium Ion Intermediate.** Consistent with the proposed intermediacy of a nitrenium ion intermediate, LFP experiments of **4a** in the presence of electron donors show that the observed intermediate undergoes electron-transfer reactions. For example, LFP of **4a** in the presence of dimethylaniline (DMA) or dimethoxybenzene (DMB) shows transients corresponding to the carbazolyl radical **6** and the cation radical of the donor, see Scheme 2.

Figure 4 shows the transient spectrum of **4a** in the presence of DMA (see Supporting Information for LFP of **4a** in the presence of DMB). The peak at 470 nm is readily assigned to the known absorption of the radical cation of DMA and the peaks at 570 and 620 to the carbazolyl radical **6**. The reference spectrum of the carbazolyl radical was obtained by LFP of *N*-nitrosocarbazole in  $\text{CH}_3\text{CN}$  which gave absorption bands at 570 and 620 nm that are qualitatively indistinguishable from a previously published spectrum of this radical.<sup>30</sup>

Previous studies by Bogdal<sup>24,25</sup> on the photoproducts of the triphenylpyridinium precursor **4b** in the presence of mesitylene suggested that the photochemistry of **4b** derives from its triplet state because of the formation of products characteristic of radical intermediates. On the basis of his studies, we considered the possibility that the trimethylpyridinium salt **4a** might follow a similar photochemical pathway. However, we find no evidence that the photochemistry of **4a** proceeds through its triplet excited state. On the contrary, as described below, product analyses and trapping rate constants are more consistent with the intermediacy

#### SCHEME 2. Electron Transfer Between **3** and Electron Donors



of a singlet nitrenium ion than a triplet. Additionally, attempts to generate the nitrenium ion through triplet sensitization of **4a** were unsuccessful. For example, we observed no quenching of the triplet excited states of benzophenone or xanthone upon addition of **4a**. Given that benzophenone and xanthone have reasonably large triplet energies of 69 and 74 kcal/mol, respectively, this result suggests that the triplet state of **4a** is higher in energy than 74 kcal/mol and is likely not an intermediate in the photochemical pathway from direct photolysis.

One potential hazard of analyzing the photoproducts of **3** is that the nitrenium ion reacts with carbazole via electron transfer to give the carbazolyl radical **6** and the carbazolyl radical cation (see Figure 4). LFP of **4a** in the presence of carbazole gives absorptions that can be assigned to the carbazolyl radical (570 and 620 nm) and the carbazolyl radical cation **6** (660 and 720 nm),<sup>31</sup> derived from electron transfer from carbazole to the nitrenium ion **3**.<sup>32</sup> Therefore, any accumulation of carbazole or carbazole addition photoproducts could spuriously give stable products consistent with triplet radical chemistry from electron transfer between the photoproducts and **3**. In fact, while we observe no transients in the LFP spectrum of the freshly prepared triphenylpyridinium salt **4b**, after 20 pulses of 355 nm laser light on a solution of **4b** in  $\text{CH}_3\text{CN}$ , a signal corresponding to the carbazolyl radical is observed that increases in intensity with further laser photolysis. LFP of freshly replenished **4b** in the presence of carbazole likewise shows a transient consistent with the carbazolyl radical.

A simpler explanation of why triplet products are observed from photolysis of **4b** while singlet behavior is seen from photolysis of **4a** is that **4b** may undergo rapid intersystem crossing of the precursor excited singlet state to its triplet excited-state before N–N bond scission, while **4a** undergoes N–N bond scission from the excited singlet state. That is, excitation of **4b** into its excited singlet state is followed rapidly by intersystem crossing to the excited triplet state and subsequent N–N bond scission to make the triplet nitrenium ion. The triplet nitrenium ion could be too short-lived to be detected using our LFP system, or it may have too weak (or unfavorably positioned) absorption bands to be observed. This explanation agrees most closely with the results obtained by Bogdal and the lack of any observable transient species upon LFP of fresh **4b** in  $\text{CH}_3\text{CN}$ .

(30) The spectrum of the carbazolyl radical, while qualitatively similar in appearance to the proposed spectrum of the singlet nitrenium ion, can be distinguished by its much longer lifetime in  $\text{CH}_3\text{CN}$  and the more defined 570 nm peak of the radical relative to the 570 nm peak of the nitrenium ion. See Supporting Information for radical spectrum and LFP of **4a** in the presence of DMB. For a previously published spectrum, see: Dilabio, G. A.; Litwiniński, G.; Lin, S.; Pratt, D. A.; Ingold, K. U. *J. Phys. Chem. A* **2002**, *106*, 11719–11725. For a paper on the reactions of the carbazolyl radical, see: Waters, W. A.; White, J. E. *J. Chem. Soc. C: Organic* **1968**, *6*, 740–745.

(31) Shida, T. *Electronic Absorption Spectra of Radical Ions*; Elsevier: Amsterdam, 1988.

(32) Carbazole has an oxidation potential of +1.35 V in  $\text{CH}_3\text{CN}$  (SCE reference). See Nie, G.; Xu, J.; Zhang, S.; Han, X. *J. Appl. Electrochem.* **2006**, *36*, 937–944.

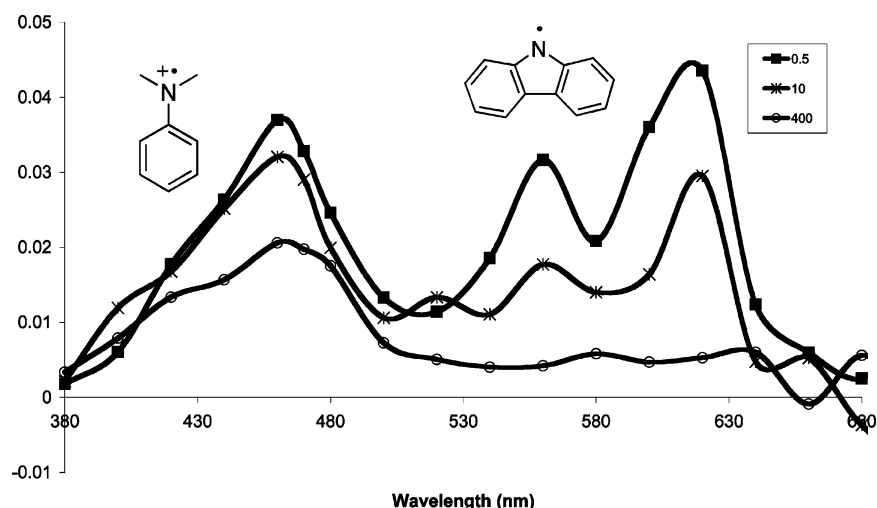
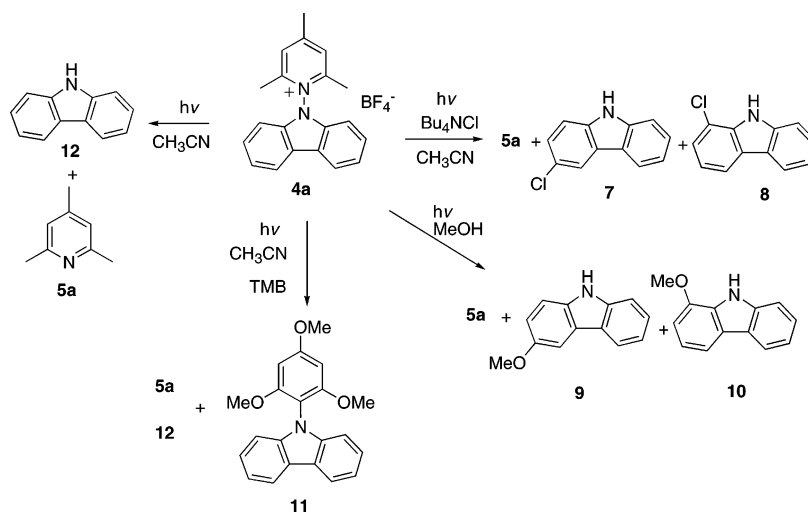


FIGURE 4. LFP of **4a** in the presence of DMA. Time scale in  $\mu\text{s}$ .

### SCHEME 3. Trapping Product Studies of **4a**



**Product Studies.** Analysis of the products obtained from photolysis of **4a** in the presence of traps is consistent with the intermediacy of a singlet nitrenium ion (Scheme 3). While triplet nitrenium ions react primarily by hydrogen atom abstraction reactions, the hallmark experiment for closed-shell singlet aryl nitrenium ions is their reaction with nucleophiles in the *ortho* and *para* positions of the aromatic ring. Consistent with the chemistry of other closed-shell singlet aryl nitrenium ions, when the photolysis of **4a** is carried out in solvent methanol, two methoxy adducts are obtained. These adducts are 3-methoxycarbazole **9** and 1-methoxycarbazole **10** as identified by comparison (TLC, GC, GC-MS) with authentic samples (in approximately a 64:36 ratio of the 3-chlorocarbazole to 1-chlorocarbazole based on GC area percent). Similarly, two chloro adducts are obtained when **4a** is photolyzed in the presence of chloride ion (as *n*-Bu<sub>4</sub>NCl) in CH<sub>3</sub>CN. One of the chloro adducts is definitively identified as 3-chlorocarbazole **7** by comparison (TLC, GC, GC-MS) with an authentic sample; the identity of the other chloro adduct has not been rigorously established but is presumed, by analogy to the reactivity of the carbazolyl nitrenium ion with methanol (and the known reactivity of other singlet aryl nitrenium ions with chloride), to be the 1-adduct **8** resulting from addition of chloride to the 1 position of the

carbazole (in approximately a 60:40 ratio of the 3-chlorocarbazole to the 1-chlorocarbazole based on GC area percent).

One principal covalent adduct **11** is obtained when **4a** is photolyzed in the presence of the pi nucleophile 1,3,5-trimethoxybenzene (TMB), resulting from addition of the aromatic ring of TMB to the carbazole nitrogen.<sup>33</sup> This result is surprising in light of the previously reported finding that diphenylnitrenium ion gives predominantly covalent adducts of TMB to the *ortho* and *para* carbons of the nitrenium ion rather than to nitrogen (30% *N* adduct, 66% *o/p* ring adducts for Ph<sub>2</sub>N<sup>+</sup>).<sup>29</sup> The selective *N*-addition of TMB to **3** may be due in part to the forced planarity of the carbazole ring that could lead to more favorable rates for *N* addition than with the diphenylnitrenium ion, which opts to twist out of plane to minimize steric repulsion. Additionally, computations predict a high localization of positive charge on the nitrogen in the carbazolyl nitrenium ion (discussed in more detail below).

(33) Based on photolysis performed using 350 nm bulbs; 254 nm photolysis gave a complex mixture of products including 5 carbazole-collidine isomers, carbazole, collidine, and 2 TMB adducts. Many of these products from 254 nm photolysis presumably arise from secondary photolysis, chemistry resulting from excitation of TMB, or reactions with accumulated photoproducts.



**TABLE 1.** Comparison of Trapping Rate Constants between **4a** and  $\text{Ph}_2\text{N}^+$ 

trap	rate constant for trapping ( $\text{M}^{-1}\text{s}^{-1}$ )	rate constant for trapping $\text{Ph}_2\text{N}^+$ ( $\text{M}^{-1}\text{s}^{-1}$ )
MeOH	$9.8 \times 10^8$	$5.2 \times 10^6$
1,3,5-Trimethoxybenzene	$9.5 \times 10^9$	$3.1 \times 10^9$
$\text{Bu}_4\text{NCl}$	$3.5 \times 10^{10}$	$1.0 \times 10^{10}$
1,4-cyclohexadiene	$9.1 \times 10^9$	$6.5 \times 10^6$

**Trapping Rate Constants.** For several traps, pseudo first-order trapping rate constants were also obtained (see Table 1). The nitrenium ion **3** reacts with both  $n$  and  $\pi$  nucleophiles at or near the diffusion limit. For example, the trapping rate constants for methanol, chloride, and 1,3,5-trimethoxybenzene were found to be  $9.8 \times 10^8$ ,  $3.5 \times 10^{10}$ , and  $9.5 \times 10^9 \text{ M}^{-1}\text{s}^{-1}$ , respectively.<sup>34</sup> Additionally, 1,4-cyclohexadiene (CHD) was found to react near the diffusion limit with a rate constant of  $9.1 \times 10^9 \text{ M}^{-1}\text{s}^{-1}$ . The latter trap can serve as both a hydrogen atom donor (BDE = 74 kcal/mol<sup>35</sup>) or as a hydride donor depending on the reactivity of the nitrenium ion.<sup>36</sup> To distinguish between these two possibilities, a full transient LFP spectrum in the presence of excess CHD was obtained. If CHD were reacting as a hydrogen atom donor, one would expect to observe transients corresponding to the carbazolyl radical cation. However, no such transients were observed upon LFP of **4a** in the presence of CHD. Given this negative result, it seems more likely that CHD is reacting as a hydride donor rather than a hydrogen atom donor.

Comparison of these trapping rate constants to previously reported rate constants for trapping of the diphenylnitrenium ion in  $\text{CH}_3\text{CN}$  suggests that the carbazolyl nitrenium ion **3** is a significantly more reactive species. Particularly noteworthy is that both methanol and 1,4-cyclohexadiene react with the carbazolyl nitrenium ion roughly 3 orders of magnitude faster than with the diphenylnitrenium ion. One possible explanation for these faster rates is that the destabilizing antiaromatic character of **3** (discussed in more detail below) leads to more favorable rates for nucleophilic attack and hydride transfer than with the diarylnitrenium ions. Alternatively, the forced planarity of **3** might lead to slightly more favorable rates for hydride transfer through less steric crowding of the nitrogen as compared to diphenylnitrenium ion.

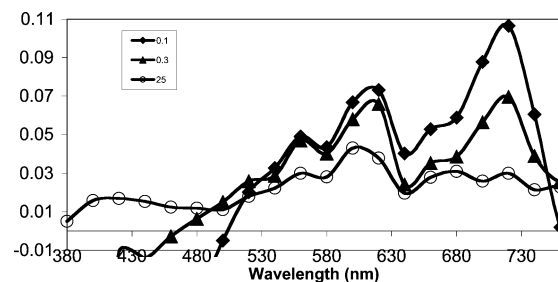
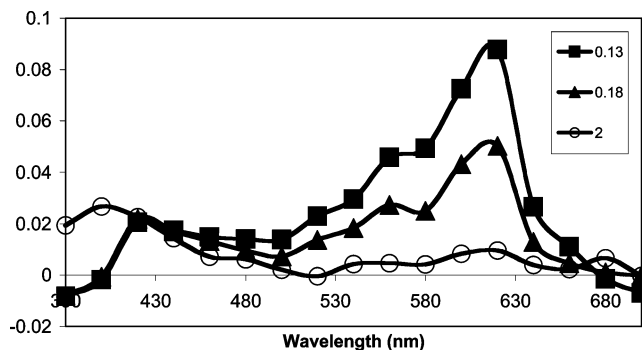
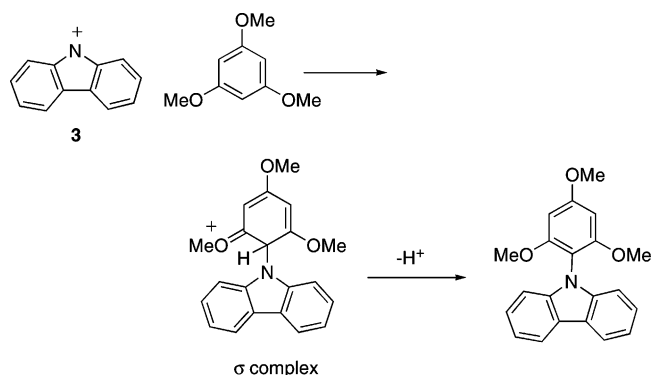
As further evidence of the chemical similarity to the diarylnitrenium ions, the carbazolyl nitrenium ion forms observable sigma adducts in the presence of  $\pi$  nucleophiles. In particular, LFP of **4a** in the presence of 1,3,5-trimethoxybenzene (TMB) gives rise to a weakly absorbing long-lived transient at 400 nm in  $\text{CH}_3\text{CN}$  (Figure 6).<sup>37</sup> We assign this transient to the sigma

(34) This rate constant for chloride trapping is slightly larger than the estimated diffusion limit for  $\text{CH}_3\text{CN}$  ( $1.8 \times 10^{10} \text{ M}^{-1}\text{s}^{-1}$ ). This anomaly could be explained by errors arising from obtaining trapping rate constants for a transient with a lifetime just inside the detection limit of our laser. Alternatively, it has been shown that the Stokes–Einstein–Smoluchowski equation often underestimates  $k_{\text{diff}}$  by a factor of  $\sim 2$  due to assumptions about the radii of the reacting species.

(35) Hawari, J. A.; Engel, P. S.; Griller, D. *Chem. Kinet.* **1985**, *17*, 1215–1219.

(36) Thomas, S. I.; Falvey, D. E. *J. Org. Chem.* **2006**, *72*, 4626–4634.

(37) The largest absorption band for this type of sigma complex has been previously observed for addition of TMB to diarylnitrenium ions at ca. 315–345 nm in  $\text{CH}_3\text{CN}$  and for the halogenated diarylnitrenium ions at 400–420 nm. See Thomas, S. I.; Falvey, D. E. *J. Org. Chem.* **2006**, *72*, 4626–4634, and McIlroy, S.; Falvey, D. E. *J. Am. Chem. Soc.* **2001**, *123*, 11329–11330.

**FIGURE 5.** LFP of **4a** in the presence of carbazole. Time scale in  $\mu\text{s}$ .**FIGURE 6.** LFP of **4a** in the presence of TMB. Time scale in  $\mu\text{s}$ .**SCHEME 4.** Addition of TMB to the Nitrenium Ion

complex resulting from nucleophilic addition of the  $\pi$  nucleophile to the nitrenium ion, see Scheme 4. One might expect that the lifetime of the sigma complex would decrease in more basic media (such as added pyridine) because of an accelerated rate of deprotonation. This is indeed the case, as the lifetime of the 400 nm transient decreases proportionally to the amount of pyridine added to the solution.

**Computed Singlet–Triplet Gaps.** The energies of the singlet and triplet states of nitrenium ions **1–3** were computed using density functional theory (DFT) to obtain the adiabatic singlet–triplet energy gaps ( $\Delta E_{\text{ST}}$ ). The merits of DFT as a method for obtaining good quantitative estimates of the singlet–triplet gaps for nitrenium ions and other hypovalent species have been discussed elsewhere.<sup>38–41</sup> All three intermediates are predicted

(38) Winter, A. H.; Falvey, D. E.; Cramer, C. J. *J. Am. Chem. Soc.* **2004**, *126*, 9661–9668.

(39) Cramer, C. J. *Essentials of Computational Chemistry: Theories and Models*, 2nd ed.; John Wiley & Sons: Chichester, 2004.

(40) Cramer, C. J.; Truhlar, D. G.; Falvey, D. E. *J. Am. Chem. Soc.* **1997**, *119*, 12338–12342.

(41) McIlroy, S.; Cramer, C. J.; Falvey, D. E. *Org. Lett.* **2000**, *2*, 2451–2454.

TABLE 2. Singlet–Triplet Gaps

Structure Number	$\Delta E_{ST}$ (B3LYP/6-31G(d,p))
1	–2.3, –2.3 <sup>a</sup>
2	–5.8
3	–7.8

<sup>a</sup> B3LYP/6-311G(2d,p)//B3LYP/6-31G(d,p).

to be ground state singlets, with the pyrrolyl nitrenium ion **1** predicted to have the smallest singlet–triplet energy splitting of –2.3 kcal/mol (a negative value indicates a singlet ground state). Benzannulation of the pyrrolyl nitrenium ion **1** to obtain **2** and **3**, as might be expected, alters the singlet–triplet gap in favor of the singlet, giving  $\Delta E_{ST}$  values of –5.8 and –7.8 kcal/mol, respectively (see Table 2).

#### Electron Configuration of the Observed Nitrenium Ion.

While all of the reactivity of the observed transient is similar to the reactivity seen for previously characterized closed-shell  $n^2$  nitrenium ions, three observations are suggestive of an  $n,p$  open-shell singlet diradical configuration.

First, the absorption spectrum of the nitrenium ion transient is very similar to that of the carbazolyl radical, with both intermediates having absorption maxima at 570 and 620 nm ( $\pm 5$  nm) in  $\text{CH}_3\text{CN}$  (the two species can be distinguished from each other by the much longer lifetime and more defined 570 nm absorption of the radical). Assuming that the absorption bands derive principally from excitations of pi electrons, one would expect that the closed shell singlet carbazolyl nitrenium ion and the carbazolyl radical would have very different absorption spectra. On the other hand, this same assumption leads to the prediction that the open-shell  $n,p$  diradical carbazolyl nitrenium ion would have an absorption spectrum very similar to the carbazolyl radical as a result of having the same electron occupation of the pi orbitals.

Second, the decay of the transient appears to be first order (see Figure 3). While the diphenylnitrenium ion ( $\text{Ph}_2\text{NH}^+$ ) has a facile unimolecular decay channel in the form of a Nazarov-like cyclization ( $\tau = 1.5 \mu\text{s}$ ) to ultimately form carbazole,<sup>42</sup> no such decay channel presents itself for the closed-shell singlet carbazolyl nitrenium ion. Despite this lack of an obvious decay channel, the carbazolyl nitrenium ion has a much shorter lifetime ( $\tau = 0.3 \mu\text{s}$ ) than  $\text{Ph}_2\text{N}^+$  in solution. The lifetime of the carbazolyl nitrenium ion transient is the same in  $\text{CH}_3\text{CN}$  and  $\text{CH}_2\text{Cl}_2$  (suggesting that the decay does not involve solvent) and is insensitive to the presence of oxygen, laser intensity (and thus the concentration of nitrenium ions), and concentration of the precursor **4a**. The isolable photoproducts in the absence of traps were found to be carbazole and collidine (27% yield of carbazole and ca. 100% yield of collidine after 54% decomposition of a 0.01 M **4a** solution in  $\text{CH}_3\text{CN}$ ). The remaining uncharacterized product(s) is an insoluble residue that is presumably poly(carbazole) oligomers similar to those seen for diphenylnitrenium ion from reaction of the nitrenium ion with accumulated photoproducts.<sup>42,43</sup>

Last, while previously reported time-dependent density functional theory (TD–DFT) calculations of diphenylnitrenium ion and its halogen-substituted analogs give predicted absorption band locations in good agreement with those found from experiment,<sup>28</sup> the predicted bands for the carbazolyl nitrenium ion do not match well with the observed spectrum of the

carbazolyl nitrenium ion. In the previous study, TD–DFT calculations predicted absorptions at 645, 637, and 647 nm for the diphenylnitrenium ion, 4,4'-dichlorodiphenylnitrenium ion, and 4,4'-dibromodiphenylnitrenium ion, respectively, close to the experimentally found absorptions of 640, 670, and 690 nm. Also of relevance, TD–DFT predicts absorption bands for the carbazolyl radical at 643 and 525 nm, in reasonable agreement with the observed bands at 620 and 570 nm. However, a TD–DFT calculation (B3LYP/6-311G(d,p)) on the closed-shell singlet carbazolyl nitrenium ion gives predicted absorption bands at 249 and 488 nm, in poor agreement with the observed absorptions at 570 and 620 nm.

Few reasonable decay pathways can be proposed that are consistent with these results and the identity of the transient as the closed-shell  $n^2$  singlet nitrenium ion. One possibility is that the nitrenium ion **3** decays to give a nitrenium ion of a different electron configuration that has unfavorable absorption properties or absorption bands outside the detection window of our LFP spectrometer. For example, the singlet nitrenium ion could undergo intersystem crossing to give the triplet carbazolyl nitrenium ion. This possibility is unlikely given that DFT predicts the closed-shell singlet to be the ground state with a reasonably large energy gap (7.8 kcal/mol) to the triplet state. (Further, when DFT errs in predicting the singlet–triplet gap, it is almost always by overly favoring the triplet state.) Another possibility is that the closed-shell nitrenium ion decays to give a different singlet state configuration of **3**. This possibility is also not supported by calculations, however, as both DFT (B3LYP) and small basis-set CASSCF(10,10)/3-21G calculations predict the closed-shell singlet state to be the lowest energy singlet electron configuration. The closed-shell singlet DFT wavefunction was found to be stable with respect to breaking orbital symmetry (restricted  $\rightarrow$  unrestricted stability), and CASSCF predicts that the lowest energy singlet configuration consists of primarily the  $n^2$  singlet state (0.82 determinant weight). On the other hand, if the observed transient is the  $n,p$  singlet excited state, an obvious unimolecular decay pathway is relaxation to the  $n^2$  singlet ground state. While a lifetime of  $\sim 0.3 \mu\text{s}$  is unusually long for an excited state, such a configurational change would be expected to be slow for the carbazolyl nitrenium ion because the change in orbital angular momentum resulting from the electron switching from the p to the n orbital is not similarly compensated by a change in spin angular momentum. In terms of chemical reactivity, however, the lifetime of the observed transient nitrenium ion is short, and product formation could arise from either the excited  $n,p$  singlet state or from the ground ( $n^2$ ) singlet state depending on the concentration and reactivity of the trap.

Thus, while the product studies, trapping rate constants, and LFP spectra in the presence of traps leave little doubt that the observed transient is a singlet nitrenium ion, the specific electronic configuration of the observed singlet nitrenium ion is less certain. The absorption spectrum and the first-order decay kinetics are most consistent with the detection of an excited  $n,p$  singlet state that relaxes to a lower-energy  $n^2$  state. However, the observed reaction products (which may arise from both states) are not qualitatively distinct from those products formed from previously characterized  $n^2$  singlet diarylnitrenium ions. Given this consideration, along with our inability to directly detect any intermediates following the decay of the nitrenium ion, the current evidence for this transient being the  $n,p$  singlet carbazolyl nitrenium ion should be considered suggestive rather than definitive.

(42) Kung, A. C.; McIlroy, S.; Falvey, D. E. *J. Org. Chem.* **2005**, *70*, 5283–5290.

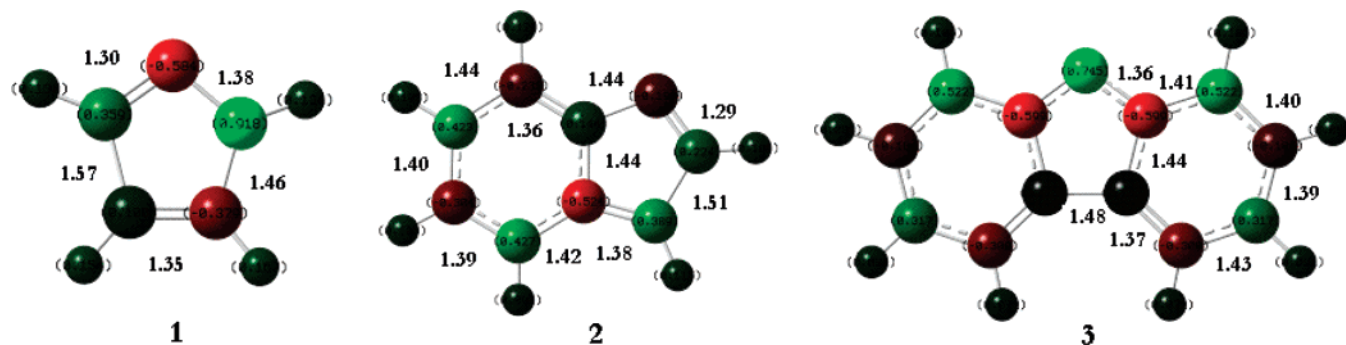


**FIGURE 7.** Bond lengths (Å) and APT charges for singlet states of **1**, **2**, and **3**. Fixed charges range from  $-1$  (bright red) to  $+1$  (bright green).

Part of the difficulty in determining a specific state assignment is that it is currently unclear whether an open-shell singlet  $n,p$  nitrenium ion would give products distinct from a closed-shell  $n^2$  singlet nitrenium ion. While to our knowledge no open-shell singlet nitrenium ion has been reported, certain aryl nitrenes (Ar–N) have open-shell singlet states lower in energy than the closed-shell singlet states.<sup>43</sup> Unfortunately, the reactivity of these species offer little insight into the potential reactivity of an open-shell singlet nitrenium ion, as open-shell singlet aryl nitrenes typically decay by formation of diazirines, followed by ring expansion to didehydroazepines.<sup>44</sup> The reactivity of open-shell singlet carbenes is likely more relevant to nitrenium ions than the reactivity of nitrenes; unfortunately, there are very few reports of open-shell singlet carbenes.<sup>45</sup> Certain 1,3- and 1,4-open-shell singlet diradicals have been shown to be trapped by nucleophiles such as chloride or alcohols, providing some precedence for an open-shell species with reactivity similar to closed-shell species.<sup>46,47</sup> However, because of the paucity of open-shell diradicals similar to nitrenium ions, the chemical behavior of an open-shell singlet nitrenium ion is unclear at this time. Therefore, further experiments and computations would be necessary to rigorously identify the electron configuration of the observed singlet nitrenium ion.

**Computational Studies of Antiaromaticity.** Computational studies were performed to assess the antiaromaticity of the carbazolyl nitrenium ion and its smaller congeners **1** and **2**. As one of the central ideas of organic chemistry, the concepts of aromaticity and antiaromaticity continue to generate considerable interest and debate for various ring systems.<sup>48–51</sup> Hückel's rules, which are used to predict potentially aromatic and antiaromatic planar ring systems, postulate that ring systems containing  $4n+2$   $\pi$  electrons are aromatic and ring systems with  $4n$   $\pi$  electrons are antiaromatic. While each of the nitrenium ions **1**, **2**, and **3** is predicted to be antiaromatic by Hückel's rules, we turned to computational studies to assess the degree of antiaromaticity (if any) in each of these nitrenium ions.

Three primary measurements related to physical observables have found widespread use for describing the aromaticity or antiaromaticity of a given ring system. These include magnetic measurements such as nucleus independent chemical shifts (NICS)<sup>52</sup> and magnetic susceptibilities,<sup>53</sup> comparison of the thermodynamic stability between a closed ring system and its analogous open ring system,<sup>51</sup> and inspection of the preferred geometries of the ring.<sup>54,55</sup> While each of these criteria has debatable merit for assigning aromaticity/antiaromaticity in the absence of other evidence, there is general agreement that a

case for aromaticity or antiaromaticity can be built by looking at the results of several of these measurements in combination. We chose the following computational measures to assess the antiaromaticity of **1**, **2**, and **3**—the degree of double bond localization (or equalization) in the optimized geometries, the relative energies of the cyclic nitrenium ions versus their open-chain counterparts (as assessed by isodesmic reactions), and the nucleus independent chemical shift (NICS) values.

Typically, double bond localization and deviations from planarity are suggestive of anti-aromatic systems, whereas bond length equalization and planarity are suggestive of aromatic systems. Given these criteria, the pyrrolyl nitrenium ion **1** appears to have the most antiaromatic character and **3** the least (see Figure 7). The geometries for each of the ring systems were optimized with density functional theory (B3LYP/6-31G(d,p)). The optimized geometry of the pyrrolyl nitrenium ion shows slight puckering from planarity and highly localized double bonds, as demonstrated by alternating bond lengths around the ring. Both **2** and **3** retain double bond localization in the five-membered ring, although it is less pronounced in **2** than in **1**, and less still in **3** than **2**. Little, if any, double bond localization is seen in the six-membered rings of **2** and **3**.

If the double bonds are localized, it follows that the positive charge should be localized as well, see Figure 7. Indeed, in the pyrrole nitrenium ion **1**, most of the positive charge ( $+0.92$ ), as predicted by the APT method,<sup>56</sup> is assigned to a carbon adjacent to the nitrogen. The indolyl nitrenium ion **2** is predicted to have significant charge delocalization off the nitrogen with

(43) Borden, W. T.; Gritsan, N. P.; Hadad, C. M.; Karney, W. L.; Kemnitz, C. R.; Platz, M. S. *Acc. Chem. Res.* **2000**, *33*, 765–771.

(44) Gritsan, N. P.; Platz, M. S. *Chem. Rev.* **2006**, *106*, 3844–3867.

(45) Scheschke, D.; Amii, H.; Gornitzka, H.; Schoeller, W. W.; Bourissou, D.; Bertrand, G. *Science* **2002**, *295*, 1880–1881.

(46) Perrin, C. L.; Rodgers, B. L.; O'Connor, J. M. *J. Am. Chem. Soc.* **2007**, *129*, 4795–4799.

(47) Little, R. D.; Brown, L. M.; Masjedizadeh, M. R. *J. Am. Chem. Soc.* **1992**, *114*, 3071–3075.

(48) Schleyer, P. *Chem. Rev.* **2001**, *101*, 1115–1117.

(49) Gomes, J. A. N. F.; Mallion, R. B. *Chem. Rev.* **2001**, *101*, 1349–1383.

(50) Mitchell, R. H. *Chem. Rev.* **2001**, *101*, 1301–1315.

(51) Krygowski, T. M.; Cyranski, M. K. *Chem. Rev.* **2001**, *101*, 1385–1419.

(52) Chen, Z.; Wannere, C. S.; Corminboeuf, C.; Puchta, R.; Schleyer, P. v. R. *Chem. Rev.* **2005**, *105*, 3842–3888.

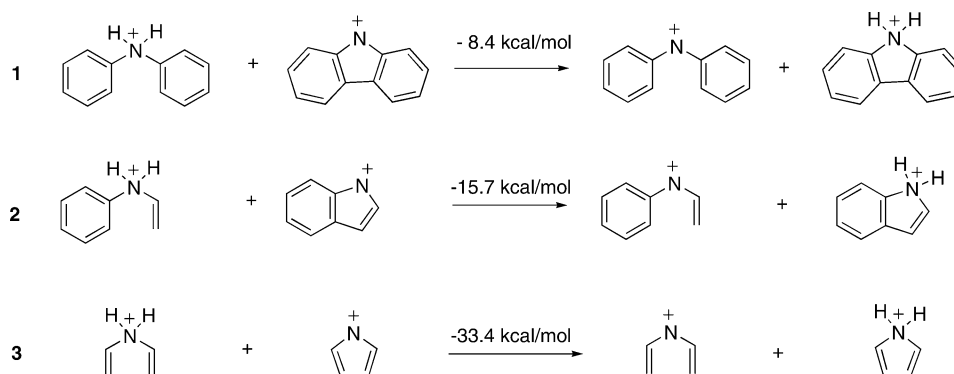
(53) Dauben, H. J.; Wilson, J. D.; Laity, J. L. *J. Am. Chem. Soc.* **1968**, *90*, 811–813.

(54) Krygowski, T. M.; Cyranski, M. K. *Tetrahedron* **1999**, *55*, 11143–11148.

(55) Katritzky, A.; Jug, K.; Oniciu, D. C. *Chem. Rev.* **2001**, *101*, 1421–1449.

(56) Cioslowski, J. *J. Am. Chem. Soc.* **1989**, *111*, 8333–8336.



SCHEME 5. Isodesmic Reactions for Hydrogen (H<sub>2</sub>) Transfer (B3LYP/6-31G(d,p))

three carbons carrying significant charge. However, the carbazolyl nitrenium ion **3** is predicted to have most of the positive charge (+0.75) reside on the nitrogen, in contrast to **1** and **2**, with nitrogens predicted to be negatively charged. This charge accumulation on the nitrogen in the carbazolyl nitrenium ion is consistent with the exclusive formation of the N-adduct of 1,3,5-trimethoxybenzene in preference to ring-substituted products.

Nucleus-independent chemical shifts are also consistent with significant antiaromatic character in each of the endocyclic nitrenium ions **1–3**. For each of the five-membered rings, the NICS values were plotted over a range of distances starting with the probe (Bq) positioned in the plane of the ring ( $r = 0$  Å) and moving it to a distance above the ring ( $r = 4$  Å) using the method recently suggested by Stanger,<sup>57</sup> with separation of the in-plane and out-of-plane contributions (Figure 8). The magnitude of the positive values for the out-of-plane components and the shape of the isotropic and out-of-plane curves for all three of these nitrenium ions are indicative of significant antiaromatic character in each of the five-membered rings. While it is tempting to use the magnitude of the NICS values to compare the relative antiaromaticities of **1–3**, it has been shown that the absolute NICS values cannot be compared for polycyclic ring systems because of the confounding effects of the neighboring rings.<sup>57</sup>

Isodesmic reactions are consistent with the geometrical predictions of **1** being the most antiaromatic and **3** the least. Ideal isodesmic reactions balance strain, resonance energy, bonds and orbitals,  $\sigma$  (anti)aromaticity, and hyperconjugation between the reactants and products, and provide estimates of the aromatic stabilization energy or antiaromatic destabilization energy for a given ring system.<sup>21,58</sup> While ideal isodesmic systems are rarely available because of difficulties in perfectly balancing these parameters (these difficulties have been appreciated in particular for charged rings<sup>21</sup>), and because of difficulties in defining appropriate reference systems, well-chosen isodesmic reactions can show trends in a series from most (anti)aromatic to least and give estimates of the (anti)-aromatic (de)stabilization energy.<sup>59</sup> We chose the three isodesmic reactions for hydrogen (H<sub>2</sub>) transfer, shown in Scheme 5, to compare the relative thermodynamic stabilities between **1**, **2**, and **3**. Hydrogen (H<sub>2</sub>) transfer rather than hydride (H<sup>−</sup>) transfer was chosen for these isodesmic reactions to avoid imbalances between the starting materials and products due to the formation of a new aromatic ring. In all cases, H<sub>2</sub> transfer

between the ring-opened amines and the nitrenium ions **1–3** was significantly favored energetically, suggesting antiaromatic character in each of these *endocyclic* nitrenium ions. Additionally, these reactions suggest that the pyrrolyl nitrenium ion **1** is the most destabilized by antiaromatic character (33.4 kcal/mol) and the carbazolyl nitrenium ion **3** the least (8.4 kcal/mol).

An alternative isodesmic reaction involving H<sub>2</sub> transfer between the pyrrolyl nitrenium ion and pyrrolidenyl nitrenium ion is shown in Scheme 6. Similar isodesmic reactions have been used to estimate the antiaromatic destabilization energy

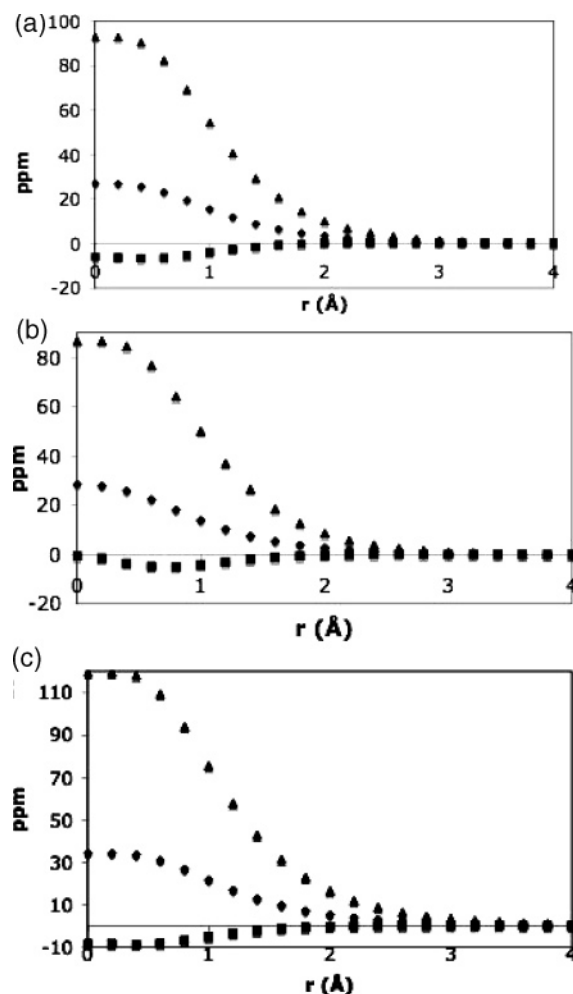


FIGURE 8. (a) **1**, (b) **2**, and (c) **3**. (▲) Out of plane component of the NICS value, (■) in-plane components, and (◆) isotropic values. All values were obtained at the center of the five-membered rings.

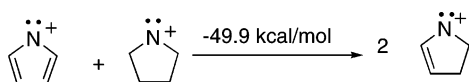
(57) Stanger, A. *J. Org. Chem.* **2006**, *71*, 883–893.

(58) Mills, N. S.; Llagostera, K. B.; Tirla, C.; Gordon, S. M.; Carpenetti, D. *J. Org. Chem.* **2006**, *71*, 7939–7946.

(59) Schleyer, P. v. R.; Puhlhofer, F. *Org. Lett.* **2002**, *4*, 2873–2876.



## SCHEME 6. Alternative Isodesmic Reaction



of cyclobutadiene.<sup>60</sup> In principle, this isodesmic reaction gives an improved balance of strain energy from starting material to product than the isodesmic reaction in Scheme 5 by constraining all structures in five-membered rings. Unfortunately, analogous isodesmic reactions for the indolyl nitrenium ion **2** or the carbazolyl nitrenium ion **3** are less desirable because of imbalances in resonance energies and aromaticity between the reactants and products. However, a significant energy difference of 16.5 kcal/mol between the isodesmic reaction shown in Scheme 6 and the isodesmic reaction in Scheme 5 suggests imbalances in one (or both) of these equations. Aside from steric imbalances, one possible explanation for the energy difference between these isodesmic reactions is that the reaction shown in Scheme 6, unlike the isodesmic reaction in Scheme 5, separates the resonance energy contribution of the two adjacent double bonds. While the differences in the energies for these two isodesmic reactions further emphasize the elusiveness of the concept of the (anti)aromatic (de)stabilization energy, and in particular the difficulty in obtaining appropriate reference systems, the qualitative conclusions that can be made from these reactions are still valid. These conclusions are that all three endocyclic nitrenium ions **1–3** are antiaromatic, and that **1** is the most destabilized by antiaromaticity and **3** the least.

In conclusion, while the carbazolyl nitrenium ion **3** is more reactive than the diphenylnitrenium ion, it shares many of the same chemical behaviors, undergoing nucleophile addition at roughly diffusion-limited rates, accepting electrons from electron-rich species, and forming  $\sigma$  complexes in the presence of the pi nucleophile trimethoxybenzene. The sum of both the computational and experimental evidence presented above suggests that the carbazolyl nitrenium ion **3** is destabilized sufficiently by antiaromatic character to make it more reactive than the diphenylnitrenium ion, but not so sufficiently as to make it favor an unusual ground state electron configuration. For the nitrenium ion observed by laser flash photolysis, spectroscopic evidence is most consistent with the assignment of an n,p singlet excited-state configuration; however, the resulting products are not sufficiently distinct from those seen for previously studied closed-shell singlet nitrenium ions to permit a definitive assignment. Experimental investigations of endocyclic nitrenium ions **1** and **2**, which are predicted by these computations to have a greater degree of antiaromaticity than the carbazolyl nitrenium ion, would be of considerable interest, as well as related endocyclic nitrenium ions with aromatic character such as those shown in Figure 9.

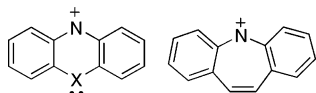


FIGURE 9. Potentially aromatic endocyclic nitrenium ions.

## Computational Methods

All calculations were performed using the Gaussian03 software package.<sup>61</sup> Geometries were optimized with density functional

theory, in particular the B3LYP functional consisting of Becke's three-parameter correlation functional<sup>62,63</sup> and Lee, Yang, and Parr's exchange functional,<sup>64,65</sup> along with the polarized double- $\zeta$  6-31G-(d,p) basis set. All optimized geometries, except where noted, were found to have zero imaginary frequencies, and the singlet states were found to be stable with respect to orbital symmetry breaking. Zero-point vibrational energy corrections were added unscaled. A preliminary CASSCF(14,13)/STO-3G calculation, which included all pi orbitals (minus the highest antibonding  $a_2$   $\pi$  orbital) and the n orbital on nitrogen in the active space, was performed on the singlet carbazolyl nitrenium ion at the DFT-optimized geometry. From this calculation, orbitals in the active space with occupations greater than 1.96 or less than 0.04 were removed for the larger basis set calculations. These included the highest remaining pi\* orbital ( $b_1$  symmetry), the n orbital ( $a_1$  symmetry), and the second pi bonding orbital ( $a_2$  symmetry). After removal of these orbitals, the remaining 10,10 active space was used for all larger basis set calculations. NICS values were computed using the GIAO method at the Hartree–Fock level with the 6-31+G(d) basis set at the DFT-optimized geometries.

## Materials/Methods

Laser flash photolysis was carried out using an ND:YAG laser that uses a harmonic generator to create an excitation beam at 355 nm. The probe beam was generated from an 350 W Xe arc lamp. Transient waveforms were digitized by a digital oscilloscope with a bandwidth of 350 MHz at a rate of 1 point per 10 ns.

Samples were prepared in CH<sub>3</sub>CN that was distilled from CaH<sub>2</sub>. Stock solutions of **4a** were prepared to have an optical density of between 1.5 and 2.0 at the excitation wavelength (355 nm). The LFP spectra were plotted from waveforms (typically 5 shot signal averaged) obtained every 10 (or 20) nm. To prevent unwanted buildup of photoproducts, the sample was replenished every 10–15 shots.

Pseudo-first-order trapping rate constants were acquired by measuring the observed decay rate constant  $k_{\text{obs}}$  for **4a** at five different concentrations of the trap. The trapping rate constant is the slope of the line made from plotting the observed rate of decay ( $k_{\text{obs}}$ ) vs the concentration of trap.

Product analysis was performed using a GC–MS equipped with an SPB-5 column (30 m, 0.25 mm). Carbazole, collidine, 1- and 3-methoxycarbazole, 3-chlorocarbazole, and 1-(carbazol-9-yl)-2,4,6-trimethoxybenzene **11** were identified by coinjection with authentic samples. Carbazole, collidine, and 3-methoxycarbazole were obtained commercially. The trimethoxybenzene adduct **11** was prepared from thermolysis of **3b** in the presence of a large excess of trimethoxybenzene in CH<sub>3</sub>CN, followed by component separation using preparatory thin-layer chromatography (15% MeOH, 85% EtOAc). 3-chlorocarbazole was made by reacting carbazole with SO<sub>2</sub>Cl<sub>2</sub> using a known procedure.<sup>66</sup>

**Acknowledgment.** We thank the Chemistry Division of the National Science Foundation for support of this work through grant CHE-0601861. H.H.G. is grateful to the Robert A. Welch Foundation for support. We thank Miriam Alexander for assistance with the generation, isolation, and characterization of compound **11** and Dr. Robin Bedford for generously donating an authentic sample of **10**. We also thank Jason Nichols for assistance using the GC–MS.

(62) Becke, A. D. *Phys. Rev. A* **1988**, 38, 3098–3100.

(63) Becke, A. D. *J. Chem. Phys.* **1993**, 98, 5648–5652.

(64) Stevens, P. J.; Devlin, F. J.; Chabalowski, C. F.; Frisch, M. J. *J. Phys. Chem.* **1994**, 98, 11632–11637.

(65) Lee, C.; Yang, W.; Parr, R. G. *Phys. Rev. B* **1988**, 37, 785–789.

(66) Bonesi, S. M.; Erra-Balsells, R. *J. Het. Chem.* **1997**, 34, 877–889.

(60) Bally, T. *Angew. Chem., Int. Ed.* **2006**, 45, 6616–6619.

(61) Frisch, M. J. T.; et al. *Gaussian03*, revision B.03; Gaussian, Inc.: Pittsburgh, PA, 2003.

**Supporting Information Available:** Full synthetic procedures.  $^1\text{H}$  and  $^{13}\text{C}$  NMR spectra for **4a** and **11**. LFP spectrum of *N*-nitrosocarbazole in  $\text{CH}_3\text{CN}$ . LFP spectrum of **4a** in the presence of 1,4-dimethoxybenzene. Details for determination of percent decomposition of **4a** and product yields in the absence of traps.

Cartesian coordinates and absolute energies for **1–3**. Full citation for reference 61. This material is available free of charge via the Internet at <http://pubs.acs.org>.

JO0708184